Am J Cancer Res 2020;10(3):1026-1044
www.ajcr.us /ISSN:2156-6976/ajcr0107617

Original Article

LPPR4 promotes peritoneal metastasis via Sp1/integrin α/FAK signaling in gastric cancer

Dan Zang[1,2,3,4*], Chuang Zhang[1,2,3,4*], Ce Li[1,2,3,4], Yibo Fan[1,2,3,4], Zhi Li[1,2,3,4], Kezuo Hou[1,2,3,4], Xiaofang Che[1,2,3,4], Yunpeng Liu[1,2,3,4], Xiujuan Qu[1,2,3,4]

[1]Department of Medical Oncology, [2]Key Laboratory of Anticancer Drugs and Biotherapy of Liaoning Province, [3]Liaoning Province Clinical Research Center for Cancer, The First Hospital of China Medical University, Shenyang 110001, China; [4]Key Laboratory of Precision Diagnosis and Treatment of Gastrointestinal Tumors, Ministry of Education, The First Hospital of China Medical University, Shenyang 110001, China. [*]Equal contributors.

Received January 9, 2020; Accepted February 20, 2020; Epub March 1, 2020; Published March 15, 2020

Abstract: Gastric cancer (GC) is one of the most common malignancies which has high incidence and mortality worldwide. Peritoneal dissemination is the main route of metastasis in advanced GC. However, few reliable diagnostic or prognostic biomarkers are available for peritoneal metastasis of GC. This study aimed to investigate the effect of lipid phosphate phosphatase-related protein type 4 (LPPR4) on the prognosis of peritoneal metastasis in GC, so as to explore the underlying molecular mechanisms and clinical significance of the process. Differentially expressed genes (DEGs) between tumor tissues and adjacent normal tissues were identified. The prognostic values of the DEGs were tested in two independent cohorts (TCGA-STAD cohort and GSE62254 cohort). Eight DEGs including LPPR4 with prognostic value in GC peritoneal metastasis were identified. The expression of LPPR4 increased in peritoneal metastasis of GC tissues, and high LPPR4 expression was associated with poor overall survival in GC. Loss- and gain-of functional experiments were performed to reveal that LPPR4 could promote the migration, invasion and adhesion abilities of GC cells in vitro. Tumor peritoneal dissemination was investigated in a mouse model to reveal that LPPR4 could promote peritoneal metastasis of GC cells in vivo. According to the Kyoto Encyclopedia of Genes and Genomics (KEGG) and gene set enrichment analysis (GSEA), LPPR4 was found to be related to focal adhesion, cell adhesion molecules (CAMs) and ECM-receptor interaction pathways. LPPR4 knockdown significantly inhibited the expression of integrin α1, integrin α2, integrin α5, integrin α6, integrin α7, p-FAK, p-Akt, p-Src and MMP2. Moreover, this process was regulated by the Specificity Protein 1 (Sp1) transcription factor. Taken together, LPPR4 plays an essential role in promoting peritoneal metastasis of GC through Sp1/integrin α/FAK signaling, and acts as a novel biomarker of prognosis of GC peritoneal metastasis. The results suggest that LPPR4 may serve as a new therapeutic target for patients with GC peritoneal metastasis.

Keywords: Gastric cancer, peritoneal metastasis, LPPR4, Sp1, integrin α

Introduction

Gastric cancer (GC) has become the 3rd leading cause of cancer-related death [1-3]. There are obvious regional differences in the incidence of GC with more than 50% of cases occurring in East Asia, especially China [4]. Although therapeutic strategies including surgery, chemotherapy, radiotherapy, immunotherapy and targeted therapy have been applied in GC, the 5-year survival rate of GC remains poor, partly due to failure to detect the early gastrointestinal symptoms of GC.

The peritoneum is the most common metastatic organ in advanced GC and peritoneal dissemination often causes large amounts of ascites or intestinal obstruction. The prognosis of patients with GC peritoneal metastasis is poor with a median survival of 7 months due to the rapid evolvement of disease, and resistance to a variety of therapies [5]. However, potent therapies for GC peritoneal metastasis have not yet been defined. There is an urgent need to better understand the underlying molecular mechanisms that drive tumorigenesis and progression in peritoneal metastasis of GC, so sensitive biomarkers for early diagnosis and more efficient therapies are required to be developed.

Lipid phosphate phosphatase-related protein type 4 (LPPR4), also known as plasticity-related

gene-1 (PRG-1), was the first identified member of a family of six transmembrane proteins that are enriched in the brain. The other four members, namely LPPR1/PRG-3, LPPR2/PRG-4, LPPR3/PRG-2, LPPR5/PRG-5, have a high degree of homology to LPPR4/PRG1 and were predicted by *in silico* analysis [6-8]. LPPRs are highly homologous to the lipid phosphate phosphatase (LPP) family proteins, owing to their similar structural and functional characteristics. LPPRs can be classified as a novel part of LPP superfamily. LPPs are a family of integral membrane glycoproteins which dephosphorylate a variety of bioactive lipid phosphates including lysophosphatidic acid (LPA) and sphingosine 1-phosphate (S1P) [9]. Bioactive lipid phosphates play a key role in initiating signaling cascades in diverse cellular activation processes. Extracellular LPA and S1P are associated with stimulated wound repair, tumor progression and metastasis [10]. The concentrations of bioactive LPA and S1P are high in ascites from patients with ovarian cancer, indicating an important role in the peritoneal metastasis of ovarian cancer [11-13]. However, the exact roles and underlying mechanisms of LPPRs/PRGs in tumorigenesis and progression remain unclear.

LPPR4 is a transmembrane protein which has 763 amino acid residues and a molecular mass of 82,983 Da. Notably, LPPRs including LPPR4, lack critical amino acids in the conserved position important for ecto-enzymatic phosphatase activity for LPPs. Furthermore, LPPR4 has an additional long hydrophilic C-terminal tails of about 400 amino acids [10]. Therefore, we speculated that LPPR4 may be more likely to display a distinguishable function and mechanism from LPPs. A previous study has shown that postsynaptic LPPR4 controls hippocampal excitability at glutamatergic synapses via presynaptic LPA receptors [14]. Moreover, LPPR4 can act as a novel calmodulin-binding protein involved in the postsynaptic compartment regulated by Ca^{2+}-dependent signaling [15]. Previous studies suggest that LPPR4 inhibits vascular smooth muscle cell migration and proliferation induced by LPA [16]. Although the role of LPPR4 has been widely investigated in the CNS, the involvement of LPPR4 in cancer is much less well known. It has been reported that LPPR4 downregulation occurs in leukemia [17]. However, the specific functions of LPPR4 in GC peritoneal metastasis have not yet been investigated.

In the present study, we selected hub genes involved in GC peritoneal metastasis using bioinformatic methods with data from the TCGA-STAD and GSE62254 cohorts. Intriguingly, we found that the expression of LPPR4 was upregulated in peritoneal metastasis of GC tissues and high expression of LPPR4 was related to poor overall survival. Moreover, our study shows that LPPR4 could promote the migration, invasion and adhesion of GC cells to foster peritoneal metastasis via the Sp1/integrin α/FAK pathway. Taken together, our findings provide an evidence that LPPR4 promotes peritoneal metastasis of GC and can be acted as a potential prognostic biomarker for patients with GC peritoneal metastasis.

Materials and methods

Data collection and preprocessing

The mRNA expression profiles and corresponding patient clinicopathological information of GSE62254 cohort were downloaded from the GEO database (http://www.ncbi.nlm.nih.gov/geo/) and preprocessed for background correction using the RMA (Robust Multichip Average) package. Transcriptome HTSeq-counts data of TCGA-STAD and corresponding patient clinicopathological information was obtained from the Genomic Data Commons (https://portal.gdc.cancr.gov/) using the R package "TCGAbiolinks". The Ensembl ID of the gene (the mRNA encoding the protein) is annotated in GENCODE27 to generate the gene symbolic name. Select the protein-encoded gene type for the mRNA for subsequent analysis.

Identification of DEGs

DEGs between tumor and adjacent normal tissues of GC in TCGA-STAD cohort were identified using R package "edgeR" under the criteria of $P < 0.05$, FDR < 0.05 and FC≥1.5. DEGs between peritoneal relapse and non-peritoneal relapse of GC in GSE62254 cohort were identified using R package "limma" under the criteria of $P < 0.05$, FDR < 0.05 and FC≥1.5.

Cell lines and cell culture

Human gastric cell lines MGC803, BGC823, MKN45, HGC27, AGS and the normal human gastric epithelial cell line GES-1 were purchased from the Chinese Academy of Sciences (Shanghai, China). MKN7 and MKN74 were

obtained from the Japanese Collection of Research Bioresources (JCRB Cell Bank, Osaka, Japan). SNU216 was obtained from the Korea Cell Line Bank (KCLB, Seoul, Korea). The human peritoneal mesothelial cell line HMrSV5 was kindly provided by Professor Youming Peng of the Second Hospital, Zhongnan University, Changsha, China and Professor Pierre Ronco, Hospital Tenon (Paris, France). HMrSV5 cell line was originally established by using retrovirus to transfect primary human peritoneal mesothelial cells (PMCs) with SV40 large-T antigen [18]. HMrSV5 cell line has been applied to a range of researches on peritoneum [19-21]. AGS cells were cultured in F12 medium (Gibco, MA,USA) with 10% fetal bovine serum (Thermo Scientific, MA, USA). The other cell lines were cultured in RPMI-1640 medium (Gibco, MA,USA) supplemented with 10% FBS, 100 μg/mL streptomycin, and 100 U/mL penicillin. All cell lines were cultured in a humidified atmosphere of 95% air and 5% CO_2 at 37°C.

siRNA transfection

LPPR4 siRNAs, Sp1 siRNAs and negative control siRNA (NC) were purchased from ViewSolid Biotech (Beijing, China).

The sequences of siRNA were as follows: siLPPR4-1: 5'-GCGAGCAUUCAUGCCUCUATT-3'; siLPPR4-2: 5'-GCAUCACCACCACGGAAUUTT-3'; siSp1: 5'-GGCAGACCUUUACAACUCAtt-3'; NC siRNA: 5'-AATTCTCCGAACGTGTCACGT-3'.

All above siRNAs were transfected into cells using jetPRIME reagent (Polyplus) according to the manufacturer's protocol.

Antibodies and reagents

Rabbit anti-Akt (#9272S), anti-phospho-Akt (Ser473) (#9271L), anti-Src (#2110S), anti-phospho-Src (#6943S), anti-FAK (#3285S), anti-phospho-FAK (Y397) (#3281S), anti-integrin β1 (#9699S), anti-integrin β2 (#73663S), anti-integrin β3 (#13166S), anti-integrin α5 (98-204S), anti-Sp1 (#9389S) and mouse anti-β-actin (#3700S) were purchased from Cell Signaling Technology (Danvers, MA, USA). Rabbit anti-integrin α7 (ab182941), anti-integrin α2 (ab133557), anti-integrin α6 (ab97760) were purchased from Abcam (Cambridge, MA, USA). Mouse anti-integrin β4 (NBP2-37392) was from Novus Biologicals (Shanghai, China). Mouse anti-integrin α1 (MAB5676) was from R&D systems (Minneapolis, MN, USA). Mouse anti-integrin β5 (H00003693-M01) was from Abnova (Taiwan, China). Mouse anti-MMP2 (13595), anti-LPPR4 (515779), secondary goat anti-rabbit and goat anti-mouse antibodies were from Santa Cruz Biotechnology (Santa Cruz, CA, USA). Matrigel was purchased from Corning (Corning Life Science, Tewksbury, MA, USA). DID dye was purchased from Invitrogen (Carlsbad, CA, USA).

RNA isolation and quantitative real-time PCR (qRT-PCR)

Total RNA was extracted with Trizol reagent (Invitrogen, Carlsbad, CA, USA). The extracted RNA was quantified by measuring the absorbance at 260 nm and the purity of total RNA was evaluated by the absorbance ratio at 260/280 nm with a NanoDrop ND-100 spectrophotometer (NanoDrop Technologies, Rockland, DE, USA). The PrimeScript RT Reagent Kit (Takara Bio, Kusatsu, Japan) was used for mRNA reverse transcription (RT). Quantitative Real-Time PCR was carried out using SYBR Premix Ex Taq II (TaKaRa) and run on Applied Biosystems® 7500 Real-Time PCR Systems (Thermo Fisher Scientific, Waltham, MA, USA). The PCR conditions were at 50°C for 2 min, 95°C for 10 min, followed by 45 cycles at 95°C for 15 s, and 60°C for 1 min and one cycle of 95°C for 15 s, 60°C for 1 min, 95°C for 30 s, 60°C for 15 s. The 2-ΔΔCt method was used for calculating the fold change of the target RNA expression of one sample compared to the calibration sample. Transcripts of 18 s was used as the internal control. The PCR primers used were as follows: LPPR4 forward: 5'-GTATGTTTCGGGCTTGTATGC-3'; LPPR4 reverse: 5'-TCCATCACTGCTGCTACCAT-3'; Sp1 forward: 5'-CCCTTGAGCTTGTCCCTCAG-3'; Sp1 reverse: 5'-TGAAAAGGCACCACCACCAT-3'; 18S forward: 5'-CCCGGGGAGGTAGTGACGAAAAAT-3'; 18S reverse: 5'-CGCCCGCCCGCTCCCAAGAT-3'.

Construction of stable LPPR4 knocked-down cell line

Negative control and LPPR4-shRNA lentiviral particles were purchased from the Genechem (Shanghai, China). HGC27 cells were transfected with NC or LPPR4-shRNA lentiviral particles following the manufacturer's instructions. The HGC27 cells were seeded in a six-well plate

with the cell density of 5.0×10^4 cells/well on day 1. On day 2, medium containing lentivirus and HitransG P (25×; Genechem) was added at MOI of 20 into the culture. HitransG P is used to increase the transfection efficiency. After 12 h of incubation, the medium was refreshed with RPMI-1640 containing FBS and cultured for 5 days. Puromycin (2 μg/mL, cat. no. P7130; Sigma-Aldrich; Merck Millipore) was used for selection of stablely transfected cells. Knockdown efficiency of LPPR4 was evaluated by qRT-PCR and Western blotting analysis.

Overexpression plasmid transfection

LPPR4 and Sp1 overexpression plasmid and the empty vector control were designed and provided by Obio Technology Corp., Ltd. (Shanghai, China). In brief, MGC803 and MKN74 cells with a cell density of 1.0×10^5 cells/well were cultured in a six-well plate on the day before transfection. The cells were transfected with 1.5 μg LPPR4 or 2.0 μg Sp1 overexpression plasmid or the empty vector control respectively according to the manufacturer's instructions on the following day. Overexpression efficiency of LPPR4 was evaluated by qRT-PCR and Western blotting, and overexpression efficiency of Sp1 was evaluated by Western blotting.

Cell viability assays

HGC27 and MKN74 cells transfected with the LPPR4 siRNA or NC siRNA and MGC803 cells transfected with LPPR4 overexpression plasmid or the empty vector control were incubated in 96-well plates with a cell density of 4,000 cells/well for 24 hours. Then, 20 uL of MTT reagent (5 mg/mL; Sigma Chemical Co., St Louis, MO, USA) was added to each well and incubated at 37°C and 5% CO_2 for 4 h. Then the supernatant in each well was discarded and 200 μL of dimethyl sulfoxide (DMSO) was added. The 96-well plate was shaken for 5 min on a horizontal shaker. The absorbance was measured at 570 nm using a microplate reader (model 550; Bio-Rad Laboratories, Inc., Hercules, CA, USA).

Migration and invasion assays

Transwell assays were performed 48 hours after transfection using 8 μm transwell chambers (Corning Life Science, MA, USA). For migration assays, transfected HGC27, MKN74 and MGC803 cells were placed into the upper chamber at a density of 3×10^4 cells/200 μL, 2×10^5 cells/200 μL and 5×10^4 cells/200 μL with RPMI-1640 medium without FBS, respectively. RPMI-1640 supplemented with 10% FBS (500 μl) was added to the lower chamber and incubated at 37°C and 5% CO_2. For invasion assays, matrigel was melted at 4°C overnight and diluted with serum-free RPMI-1640 in a 1:30 ratio in advance. The transwell migration chambers were precoated with 50 μL matrigel on ice and incubated at 37°C for 1 hour to allow the matrigel to solidify. Transfected HGC27, MKN74 and MGC803 cells were placed into the upper chamber at a density of 4×10^4 cells/200 μL, 3×10^5 cells/200 μL and 1×10^5 cells/200 μL with RPMI-1640 medium without FBS, respectively. After 24 hours of incubation, cells remaining on the upper membrane were removed with cotton-tipped swabs while cells on the lower surface of the filter were fixed with ethanol, stained with Reiter dying for 1 min, followed by mixed Giemsa redyeing for 1 hour. The stained cells were counted and photographed by a microscope (Olympus, Tokyo, Japan) at ×200 magnification. At least five randomly selected fields were counted and analyzed statistically.

Wound healing assays

Scratch wound healing assays were operated 48 hours after transfection. HGC27, MKN74 and MGC803 cells were seeded in six-well plates until confluence and wounded by scratching a straight line with a 200 μl pipette tip. Then the supernatant in each well was aspirated and replaced with fresh medium without FBS. Migration images were captured at 0, 24 h after scratching. All experiments were performed for repeated three times. The area in the blank was analyzed and quantified with the ImageJ software and percentage was calculated according to the formula (S0-St)/S0.

Tumor cell adhesion assays

Adhesion assays were carried out 48 hours after transfection. HMrSV5 cells were seeded in six-well plates overnight to prepare a confluent monolayer. Transfected HGC27, MKN74 and MGC803 cells stained with DID dye which was diluted with serum-free RPMI-1640 medium in a 1:200 ratio for 20 minutes at 37°C were placed onto the HMrSV5 monolayer at a density of 5×10^4, 1×10^5 and 5×10^4 cells,

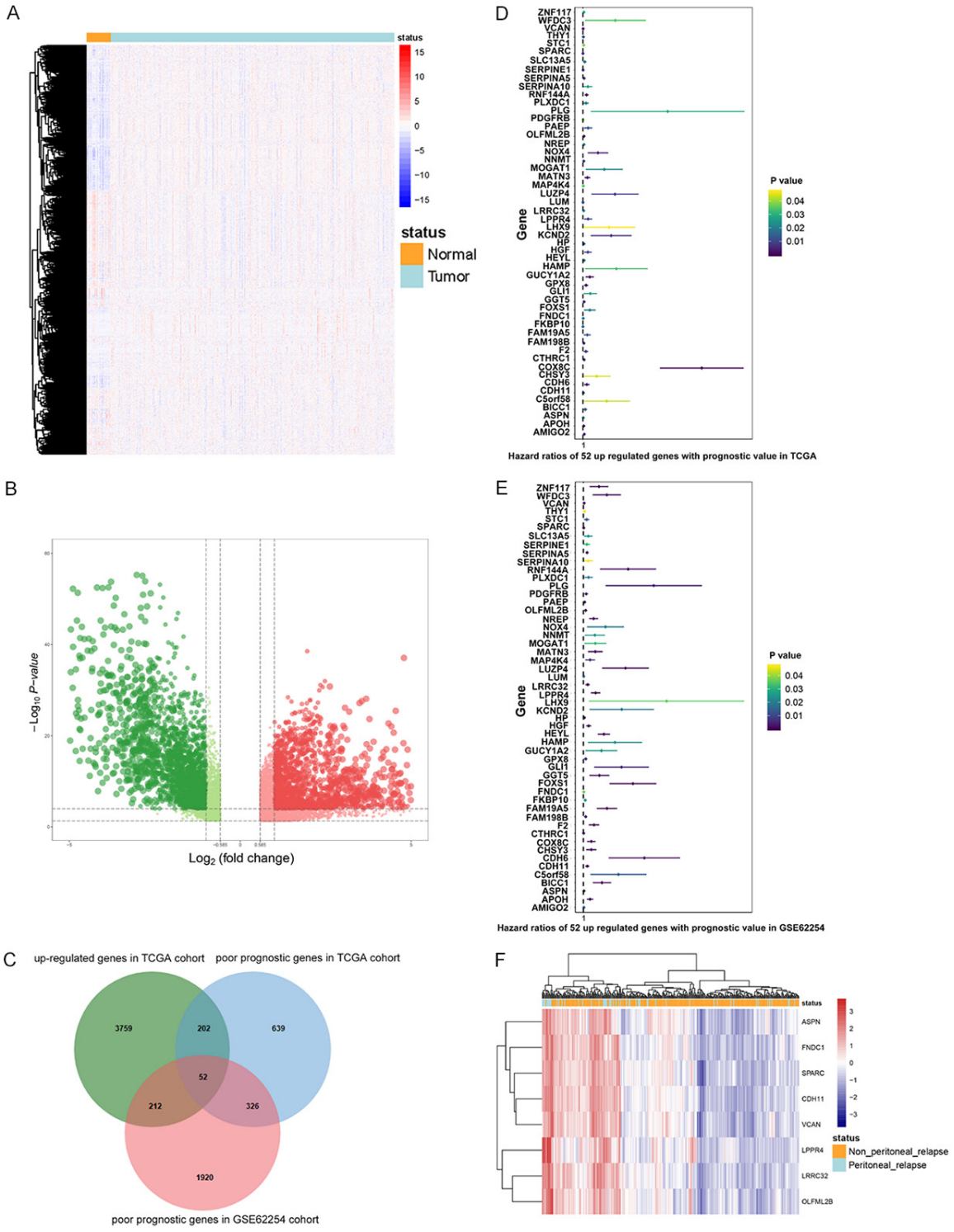

Figure 1. Identification of LPPR4 as peritoneal metastasis-related genes in GC. A, B. The heatmap and volcano map of the DEGs between cancer tissues and adjacent tissues of TCGA-STAD cohort respectively. C. Venn diagram of the selection of the 52 DEGs with stable prognostic value. D. The univariate analysis results of the 52 genes with prognostic value in TCGA-STAD cohort. E. The univariate analysis results of the 52 genes with prognostic value in GSE62254 cohort. F. The heatmap of the eight peritoneal metastasis related genes in GSE62254 cohort.

respectively. After 6 hours of incubation at 37°C, non-adherent tumor cells were washed by PBS, and adherent tumor cells were counted and photographed by a fluorescence micro-

Table 1. Eight prognostic and peritoneal metastasis-related genes in GC

Gene symbol	Gene name	logFC	*P*-value
ASPN	asporin	1.225852996	1.71E-06
LPPR4	lipid phosphate phosphatase-related protein type 4	0.874027316	2.09E-08
FNDC1	fibronectin type III domain-containing protein 1	0.7142821	0.02562204
OLFML2B	olfactomedin-like protein 2B	0.705273769	1.21E-05
CDH11	cadherin-11	0.662220922	1.27E-05
LRRC32	leucine-rich repeat-containing protein 32	0.644397024	2.30E-08
VCAN	versican core protein	0.643088221	0.000100684
SPARC	secreted protein acidic and rich in cysteine	0.639320219	2.75E-06

scope (Olympus, Tokyo, Japan) at ×100 magnification. All images were captured in at least five randomly selected fields.

Immunoprecipitation and Western blotting analysis

Cells were extracted in 1% Triton lysis buffer (1% Triton X-100, 50 mM Tris-Cl pH 7.4, 150 mM NaCl, 10 mM EDTA, 100 mM NaF, 1 mM Na_3VO_4, 1 mM PMSF, 2 μg/mL aprotinin) and quantified using the Coomassie brilliant blue method. For immunoprecipitation, cell lysates were mixed with LPPR4 antibody at 4°C for 6 hours at least. Then the mixture was added into 40 μl of protein G-sepharose beads (Cell Signaling Technology) and slowly shaken for another 2 hours at 4°C. The immunoprecipitated proteins were eluted with lysis buffer for four times and boiled by heat treatment at 95°C for 5 min with 2X sampling buffer. For Western blotting analysis, the cell lysates were separated by 8% SDS-PAGE and electrophoretically transferred to a polyvinylidene fluoride (PVDF) membrane (Millipore, Bedford, MA, USA). The membranes were blocked with 5% skim milk in tris-buffered saline Tween-20 (TBST) buffer (10 mM Tris-Cl pH 7.4, 150 mM NaCl, 0.1% Tween-20) at room temperature for 1 hour and incubated with the indicated primary antibodies overnight at 4°C. After incubating with the appropriate secondary antibodies at room temperature for 40 minutes, the protein bands were detected with enhanced chemiluminescence reagent (SuperSignal Western Pico Chemiluminescent Substrate; Pierce, USA) and visualized with the Electrophoresis Gel Imaging Analysis System (DNR Bio-Imaging Systems, Israel).

In vivo tumor peritoneal dissemination model

Ten BALB/c 4-6-week-old female nude mice were purchased from Beijing Vital River Laboratory Animal Technology Co, Ltd. and randomly allocated to two groups. All animal experiments were approved by the Institutional Review Board of China Medical University. HGC27-shNC and HGC27-shLPPR4 cells (5×10^6 in 300 μL PBS) were inoculated peritoneally. All mice were sacrificed after 8 weeks according to the criterion by the Committee on Animal Care in China Medical University and metastatic peritoneal nodules were counted and weighed.

Statistical analysis

All statistical analyses were performed using GraphPad Prism software, Social Sciences (SPSS) software version 20.0, and R software. R package survival was used to perform univariate cox analysis. False discovery rate (FDR) was calculated with R package p.adjust. GSEA was conducted by using GSEA v2.2.2 (http://www.broadinstitute.org/gsea). KEGG analysis was performed by R package clusterProfiler. R package GOplot was used to demonstrate the results of KEGG analyses. Wilcoxon test was used to analyze the association between LPPR4 expression and peritoneal recurrence. The data of cell culture experiment was displayed as means ± standard deviation (SD) of three independent experiments. Differences between two groups were assessed using the Student's t-tests. Spearman correlation analysis was used to analyze the correlations. Kaplan-Meier method and log-rank test were used to analyze the survival curves. $P < 0.05$ was considered to be statistically significant (*$P < 0.05$, **$P < 0.01$, ***$P < 0.001$).

Results

Identification of prognostic and peritoneal metastasis-related genes in GC

To obtain genes that play a vital role in the process of GC peritoneal metastasis, we first sc-

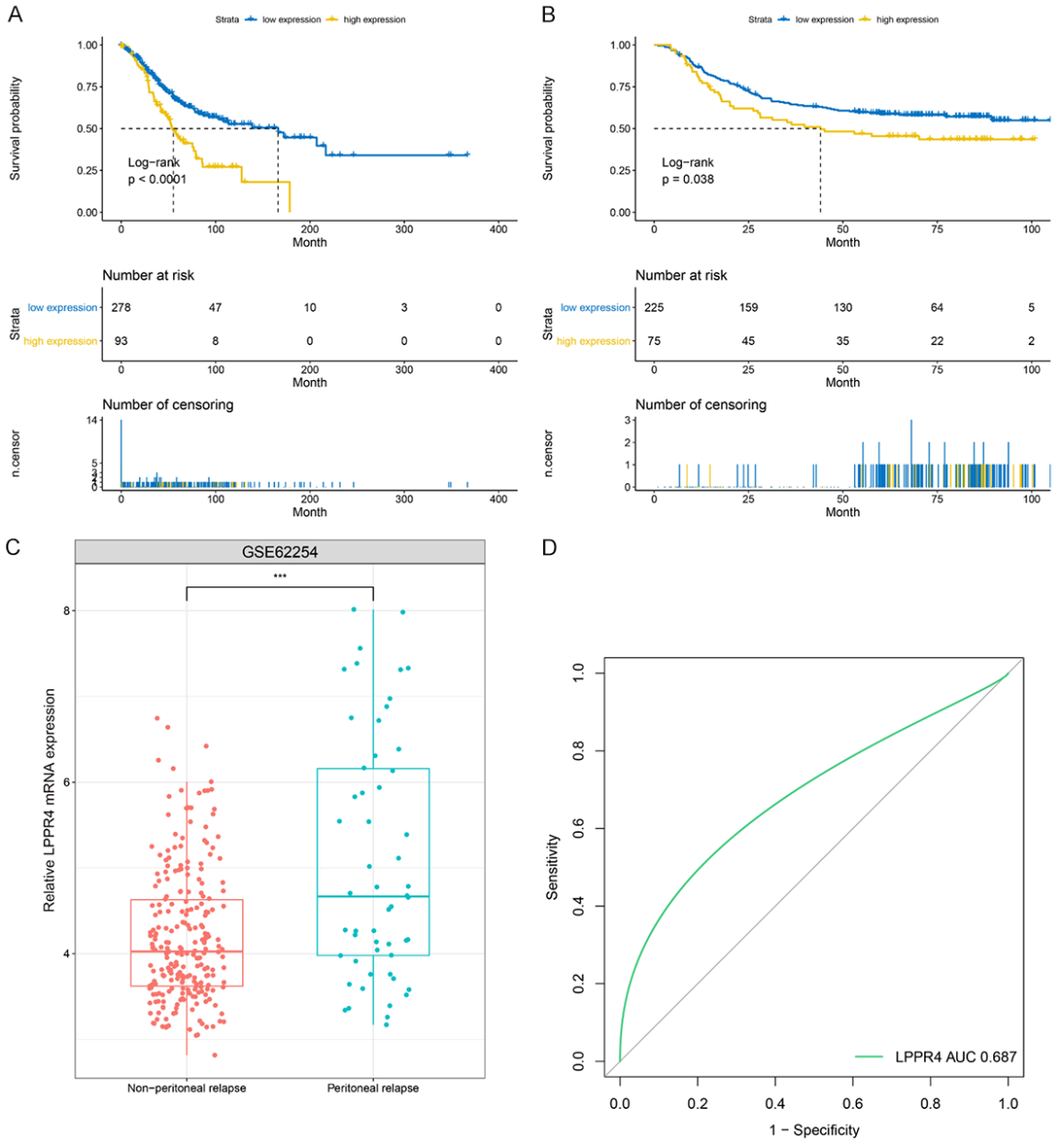

Figure 2. High expression of LPPR4 predicts poor prognosis for GC patients. A. Kaplan-Meier curve of LPPR4 expression in OS of TCGA-STAD cohort. B. Kaplan-Meier curve of LPPR4 expression in OS of GSE62254 cohort. C. LPPR4 expression in peritoneal relapse group and non-peritoneal relapse group. D. ROC curve analysis of LPPR4. *P* value was determined using *Wilcoxon test.* ***$P < 0.001$.

reened differential expression genes in TCGA-STAD cohort using R package "edgeR" with the criteria of P < 0.05, FDR < 0.05 and FC≥1.5. 4,225 genes were up-regulated in tumor tissues (**Figure 1A**, **1B**). Moreover, the prognostic values of these 4,225 genes in the TCGA-STAD and GSE62254 cohorts were tested, with the criteria of P < 0.05 and HR>1, 52 genes passed the audit (**Figure 1C-E**). Finally, to confirm the role of these 52 prognostic genes in the biological behavior of peritoneal metastasis, we conducted differential expression genes screening using the R package "limma" in GSE62254 for 54 patients with peritoneal recurrence, and 246 patients without peritoneal recurrence. A total of 502 peritoneal metastasis-associated genes were obtained under the criteria of P < 0.05, FDR < 0.05 and FC≥1.5 (Figure S1A, S1B). In summary, eight genes were identified as both prognostic and peritoneal metastasis-related genes (**Figure 1F**; **Table 1**). Notably, LPPR4 ranked the second highest according to

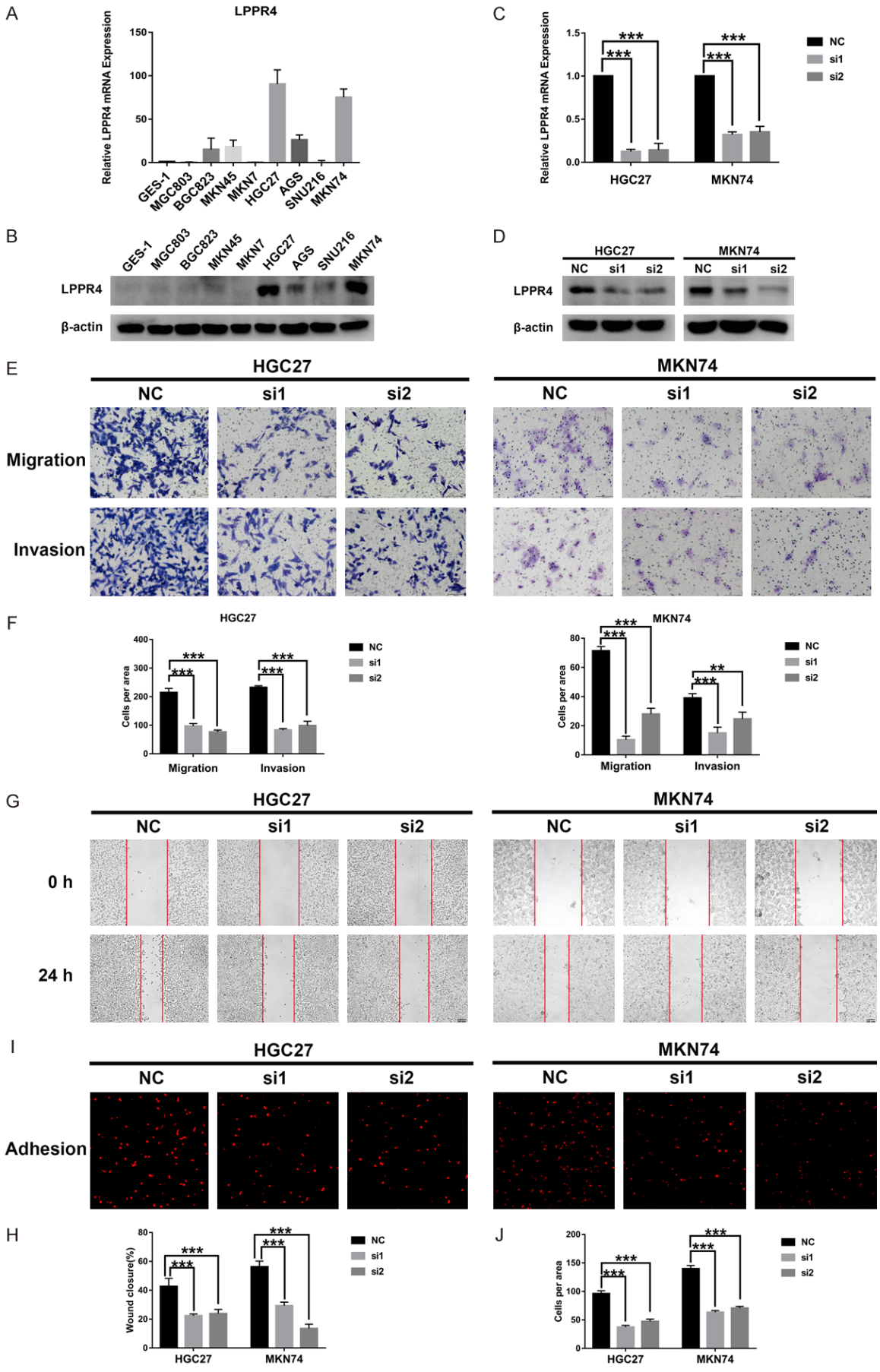
A
LPPR4
Relative LPPR4 mRNA Expression
GES-1
MGC803
BGC823
MKN45
MKN7
HGC27
AGS
SNU216
MKN74
C
Relative LPPR4 mRNA Expression
NC
si1
si2
HGC27
MKN74
B
LPPR4
β-actin
D
HGC27
MKN74
E
HGC27
MKN74
NC
si1
si2
Migration
Invasion
F
Cells per area
Migration
Invasion
G
0 h
24 h
I
Adhesion
H
Wound closure(%)
J
Cells per area

Figure 3. Knockdown of LPPR4 inhibits migration, invasion and adhesion in GC cells *in vitro*. A. LPPR4 mRNA expression in eight GC cell lines and GES-1 cells by qRT-PCR. B. Protein expression of LPPR4 in eight GC cell lines and GES-1 cells by Western blotting. C, D. HGC27 and MKN74 cells were transfected with NC-siRNA, LPPR4-siRNA-1 (si1) and LPPR4-siRNA-2 (si2). LPPR4 expression levels were detected by qRT-PCR and Western blotting analyses. E, F. Transwell migration and invasion assays of HGC27 and MKN74 cells with transient LPPR4 knockdown. Original magnification, 200×. Scale bar = 100 μm. G, H. Wound healing assays for the evaluation of LPPR4 knockdown on HGC27 and MKN74 cells migration ability. Original magnification, 50×. Scale bar = 200 μm. I, J. Adhesion assays to show HGC27 and MKN74 cells with transient LPPR4 knockdown adherent to HMrSV5 cells. Original magnification, 100×. Scale bar = 200 μm. β-actin was used as an internal reference for Western blotting. Each experiment was repeated at least three times. All the data were expressed as mean ± SD, $^{**}P < 0.01$, $^{***}P < 0.001$, based on Student's *t*-test.

fold change and might be related to tumorigenesis and progression of GC peritoneal metastasis. Therefore, LPPR4 was selected for further experimental analysis.

High expression of LPPR4 predicts poor prognosis for GC patients

The relationship between the expression level of LPPR4 and the prognosis of GC was further evaluated. Kaplan-Meier analysis was performed on the TCGA-STAD and GSE62254 cohort patients. Patients with high expression of LPPR4 in both databases were found to have significantly lower overall survival compared to patients with low expression of LPPR4 (**Figure 2A**, **2B**). Then, samples were divided into a peritoneal relapse group and non-peritoneal relapse group based on the peritoneal recurrence. A significant positive association between LPPR4 expression and peritoneal recurrence was observed in the GSE62254 cohort (**Figure 2C**). Receiver operating characteristic (ROC) curve analysis was performed to evaluate the sensitivity and specificity of LPPR4 for the diagnosis of GC peritoneal metastasis. The area under ROC curve (AUC) of LPPR4 was 0.687, demonstrating that LPPR4 has a high sensitivity and specificity for GC peritoneal metastasis diagnosis (**Figure 2D**). These results suggested that high expression of LPPR4 was related to poor prognosis for GC patients, and LPPR4 can be used as a candidate biomarker for the diagnosis and prognosis of GC peritoneal metastasis.

LPPR4 promotes migration, invasion and adhesion of GC cells to foster GC peritoneal metastasis in vitro

To investigate whether LPPR4 could promote GC peritoneal metastasis, the effect of LPPR4 on migration, invasion of GC cells and adhesion of GC cells to HMrSV5 cells was investigated using GC cell lines. To understand the biological functions of LPPR4 in GC cells, LPPR4 mRNA and protein expression were measured in eight GC cell lines, and the normal gastric epithelial cell line GES-1. LPPR4 was found to be significantly up-regulated in the GC cell lines compared to GES-1 cells (**Figure 3A**, **3B**). HGC27 and MKN74 cells were chosen for the loss of function experiments and MGC803 cells were selected for the gain of function experiments due to the highest and lowest expression levels of LPPR4 in these GC cell lines, respectively. qRT-PCR and Western blotting were used to determine the transfection efficiencies of LPPR4 siRNAs in HGC27 and MKN74 cells (**Figure 3C**, **3D**). In HGC27 and MKN74 cells, transwell migration and matrigel invasion assays showed that the migration and invasion abilities were significantly decreased in LPPR4-knockdown cells compared to the NC cells ($P < 0.01$, **Figure 3E**, **3F**), while MTT assays indicated no significant difference in proliferation effect between NC and LPPR4 siRNA cells (Figure S2A, S2B). Wound healing assays showed that knockdown of LPPR4 significantly decreased the wound healing capability compared to NC cells ($P < 0.001$, **Figure 3G**, **3H**). For adhesion assays, HMrSV5 cells were used to test the attachment of GC cells to PMCs. Interestingly, less LPPR4-knockdown GC cells were adhered to a dense layer of HMrSV5 cells compared to the control group ($P < 0.001$, **Figure 3I**, **3J**).

To further validate the biological functions of LPPR4, LPPR4 was overexpressed in MGC803 cells lines using LPPR4 overexpression plasmid and overexpression efficiency was tested by qRT-PCR and Western blotting assays (**Figure 4A**, **4B**). The migration and invasion potential of MGC803 cells was significantly enhanced in the LPPR4-overexpression group ($P < 0.05$, **Figure 4C**, **4D**), whilst no significant difference was observed in cell proliferation based on

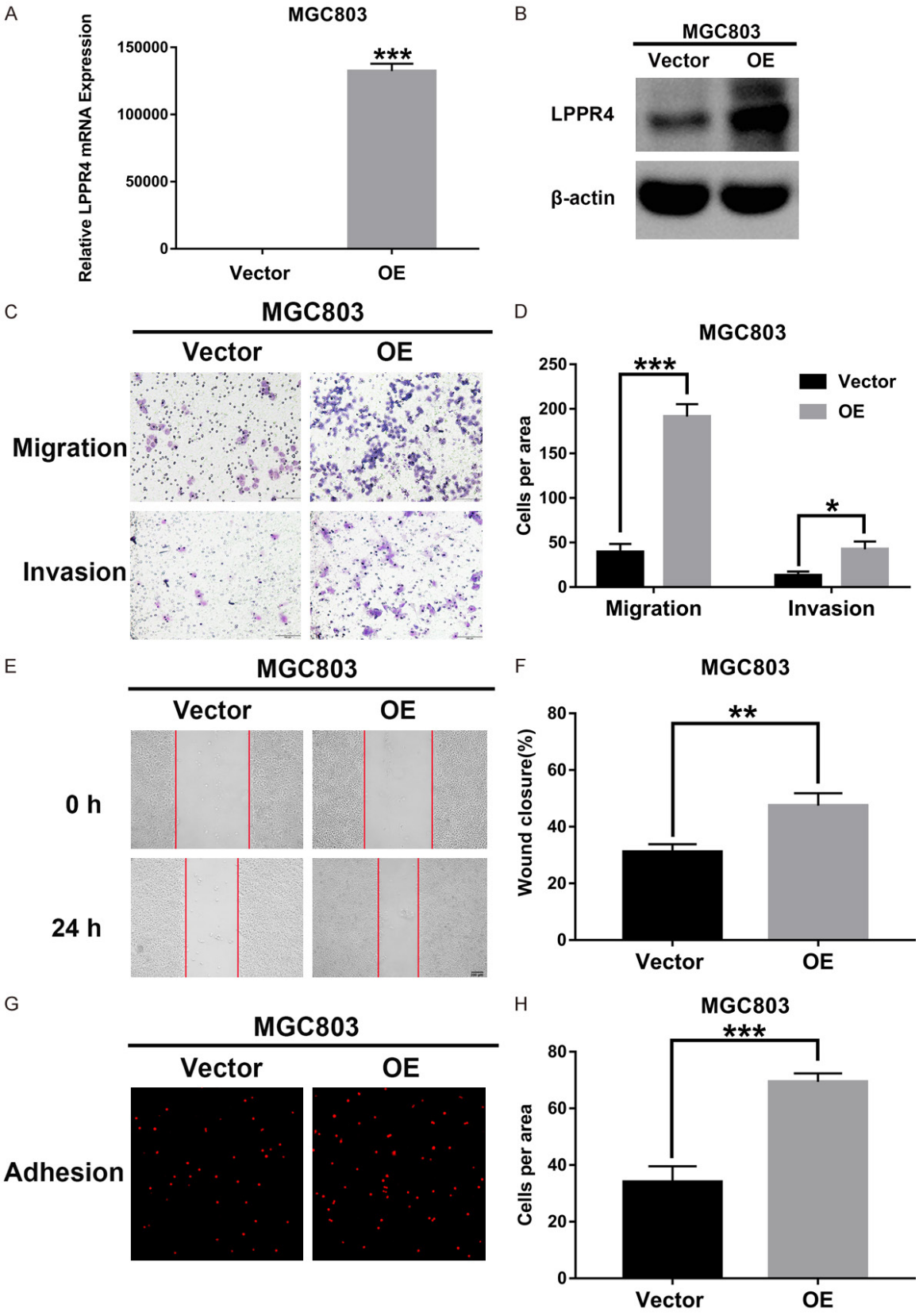

Figure 4. Overexpression of LPPR4 promotes migration, invasion, and adhesion in GC cells *in vitro*. A, B. MGC803 cells were infected with LPPR4 overexpression plasmid or the empty vector control. LPPR4 expression levels were detected by qRT-PCR and Western blotting analyses. C, D. Transwell migration and invasion assays of MGC803

cells with LPPR4 overexpression. Original magnification, 200×. Scale bar = 100 μm. E, F. The migratory abilities of MGC803 cells transfected with LPPR4 overexpression plasmid were detected by wound healing assays. Original magnification, 50×. Scale bar = 200 μm. G, H. Adhesion assays to assess MGC803 cells with LPPR4 overexpression adherent to HMrSV5 cells. Original magnification, 100×. Scale bar = 200 μm. β-actin was used as a loading control in Western blotting. Each experiment was repeated at least three times. All the data were expressed as mean ± SD, $*P < 0.05$, $**P < 0.01$, $***P < 0.001$, based on Student's *t*-test.

MTT assays (Figure S2C). Similarly, the migration and motility of MGC803 cells were significantly increased in the LPPR4 overexpression group by wound healing assays ($P < 0.01$, **Figure 4E**, **4F**). Furthermore, more LPPR4-overexpression GC cells were attached to HMrSV5 cells by adhesion assays ($P < 0.001$, **Figure 4G**, **4H**). Therefore, these results suggested that LPPR4 could promote migration and invasion of GC cells, and adhesion of GC cells to HMrSV5 cells *in vitro*.

KEGG and GSEA enrichment analysis of LPPR4

To elucidate the mechanisms of LPPR4 in peritoneal metastasis of GC, we selected 1,000 genes which were most related to LPPR4 based on Spearman's rank correlation in the TCGA-STAD data set, and conducted a KEGG enrichment analysis on these 1,000 genes. The results of KEGG enrichment analysis showed that these 1,000 genes were significantly enriched in PI3K-Akt, focal adhesion, ECM-receptor interaction, and CAMs pathways (**Figure 5A-C**). In addition, GSEA analysis was also carried out to identify the abnormally regulated pathways in GC patients. As shown in **Figure 5D** and **5E**, CAMs, ECM-receptor interaction and focal adhesion pathways were the most commonly enriched signaling pathways. Therefore, we hypothesized that LPPR4 played an important role in the adhesion process of GC cells.

LPPR4 activates transcription of integrin α through Sp1

It is well known that integrins (ITGs) play a key role in the adhesion of cancer cells to induce metastasis [22]. According to our predicted pathways, we verified several relevant members of integrin family proteins including ITGA1, ITGA2, ITGA5, ITGA6, ITGA7, ITGB1, ITGB2, ITGB3, ITGB4 and ITGB5 by Western blotting. Interestingly, the expression of ITGA1, ITGA2, ITGA5, ITGA6 and ITGA7, but not ITGB1, ITGB2, ITGB3, ITGB4 and ITGB5, were significantly down-regulated by knockdown of LPPR4. Furthermore, levels of p-FAK, p-Akt, p-Src, as well as MMP2 were dramatically decreased. Conversely, overexpression of LPPR4 exhibited the opposite regulation (**Figures 6A**, S3A). The correlation analysis in the TCGA-STAD cohort showed a positive correlation between LPPR4 and ITGA1, ITGA2, ITGA5, ITGA6, ITGA7 (Figure S3B). Then, we explored the relationship between LPPR4 and ITGA1, ITGA2, ITGA5, ITGA6, ITGA7. However, immunoprecipitation assays failed to demonstrate a direct interaction between LPPR4 and ITGA1, ITGA2, ITGA5, ITGA6, ITGA7 (**Figure 6B**). Therefore, to further investigate the mechanism by which LPPR4 up-regulated ITGA1, ITGA2, ITGA5, ITGA6 and ITGA7 expression, we analyzed ITGA1, ITGA2, ITGA5, ITGA6 and ITGA7 promoter using the UCSC genome website and JASPAR database [23], showing that Sp1 is a potential transcription factor regulator.

It was previously reported that Sp1 acted as a known transcription factor for gene expression of integrin α2 in breast cancer [24], and integrin α5 during EMT in cancer [25]. Hence, we speculated that LPPR4 might regulate the expression of ITGA1, ITGA2, ITGA5, ITGA6 and ITGA7 by modulating their transcription factor Sp1. Then, the correlations between LPPR4 and Sp1, as well as Sp1 and ITGA1, ITGA2, ITGA5, ITGA6, ITGA7 were verified in the TCGA-STAD cohort. From the correlation analysis, LPPR4 was positively related to Sp1 ($R = 0.276$; $P < 0.001$), and the expression of Sp1 was shown to be positively associated with the expression of ITG genes: ITGA1 ($R = 0.386$, $P < 0.001$), ITGA2 ($R = 0.541$, $P < 0.001$), ITGA5 ($R = 0.202$, $P < 0.001$), ITGA6 ($R = 0.615$, $P < 0.001$), ITGA7 ($R = 0.255$, $P < 0.001$; **Figure 6C**). qRT-PCR (**Figure 6D**) and Western blotting (**Figure 6E**) showed that Sp1 mRNA and protein expression were down-regulated after knockdown of LPPR4 in HGC27 and MKN74 cells. Our results were consistent with the correlation between LPPR4 and SP1 as shown previously using TCGA-STAD databases. Then, we knocked down Sp1 to examine protein levels of ITGA1, ITGA2, ITGA5, ITGA6 and ITGA7. qRT-PCR and Western blotting were adopted to verify the

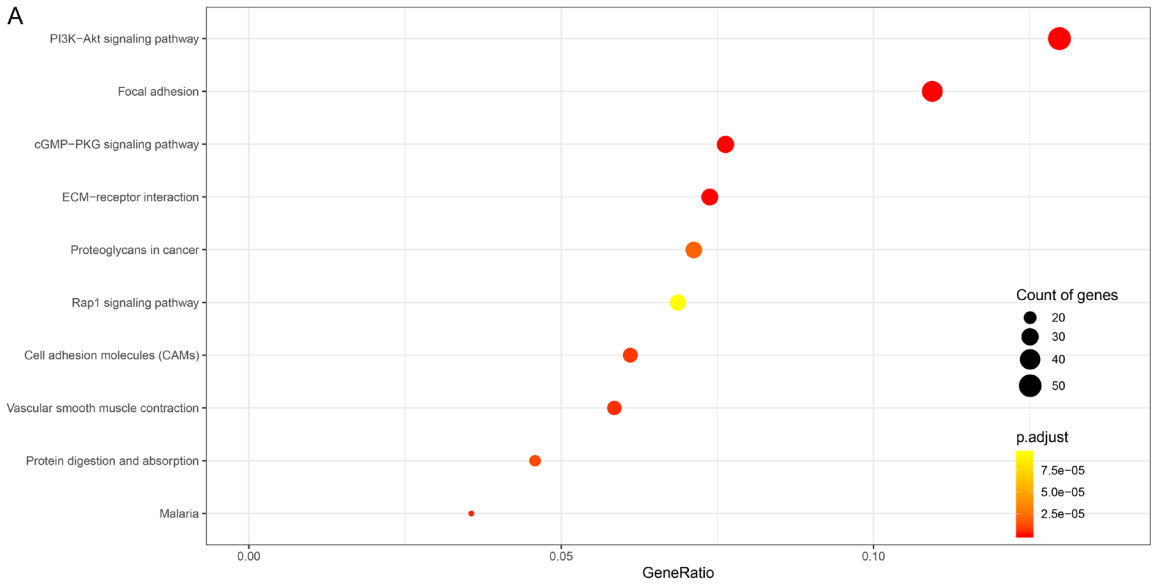
A
PI3K−Akt signaling pathway
Focal adhesion
cGMP−PKG signaling pathway
ECM−receptor interaction
Proteoglycans in cancer
Rap1 signaling pathway
Cell adhesion molecules (CAMs)
Vascular smooth muscle contraction
Protein digestion and absorption
Malaria
0.00
0.05
0.10
GeneRatio
Count of genes
20
30
40
50
p.adjust
7.5e−05
5.0e−05
2.5e−05

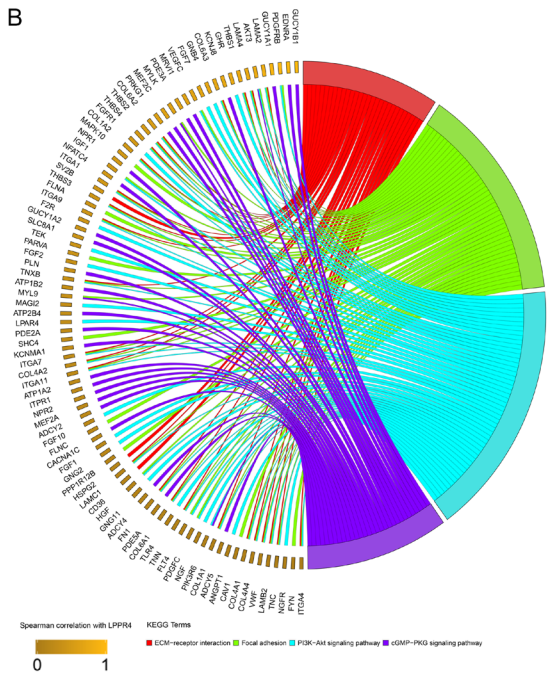
B
Spearman correlation with LPPR4
0
1
KEGG Terms
ECM−receptor interaction
Focal adhesion
PI3K−Akt signaling pathway
cGMP−PKG signaling pathway

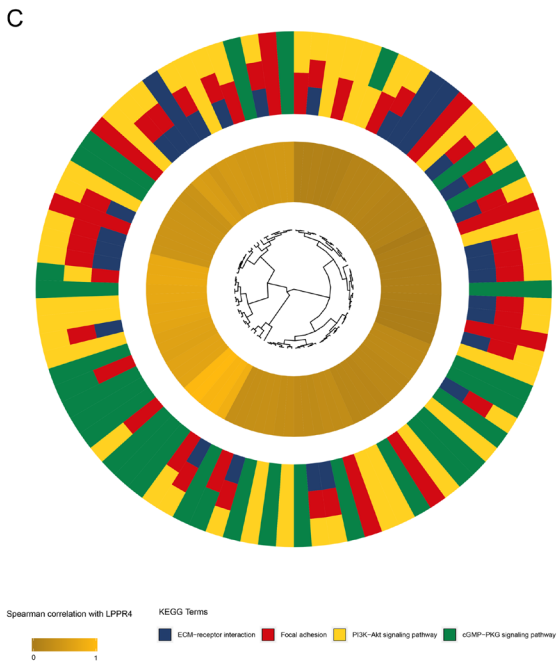
C
Spearman correlation with LPPR4
0
1
KEGG Terms
ECM−receptor interaction
Focal adhesion
PI3K−Akt signaling pathway
cGMP−PKG signaling pathway

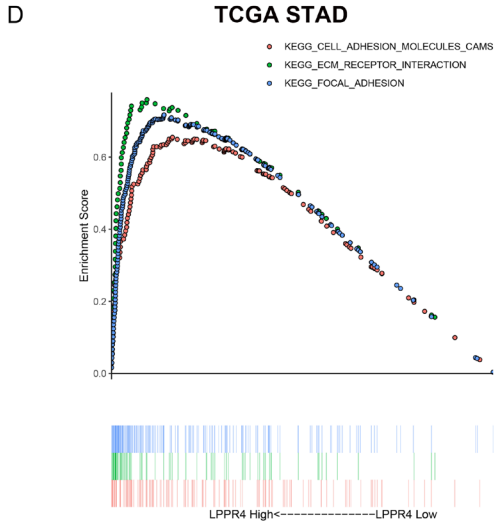
D
TCGA STAD
KEGG_CELL_ADHESION_MOLECULES_CAMS
KEGG_ECM_RECEPTOR_INTERACTION
KEGG_FOCAL_ADHESION
Enrichment Score
0.0
0.2
0.4
0.6
LPPR4 High<----------LPPR4 Low

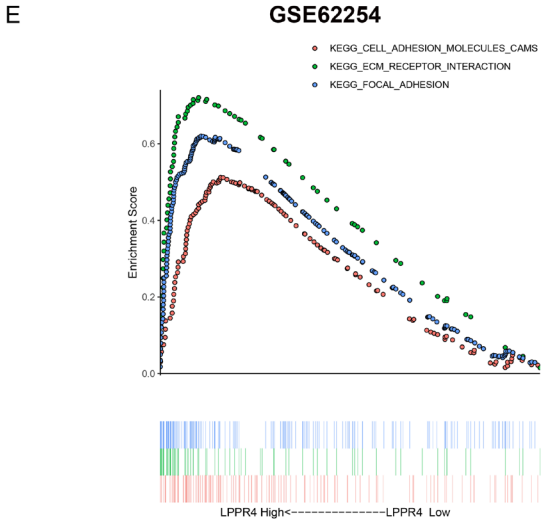
E
GSE62254
KEGG_CELL_ADHESION_MOLECULES_CAMS
KEGG_ECM_RECEPTOR_INTERACTION
KEGG_FOCAL_ADHESION
Enrichment Score
0.0
0.2
0.4
0.6
LPPR4 High<----------LPPR4 Low

Figure 5. KEGG and GSEA enrichment analysis of LPPR4. A. 1000 genes which were most relevant to LPPR4 were enriched in KEGG pathways. Fold enrichment of each KEGG term is indicated by the x-axis and bar color. B. Hierarchical clustering of gene expression profiles of each KEGG pathway. C. Chord plots show the relationship between genes and the KEGG pathway. D. GSEA terms that are significantly enriched in TCGA-STAD cohort. E. GSEA terms that are significantly enriched in GSE62254 cohort.

transfection efficiency of Sp1 siRNA in HGC27 and MKN74 cells (**Figure 6F**, **6G**). As shown in **Figure 6G**, it was found that ITGA1, ITGA2, ITGA5, ITGA6 and ITGA7 were down-regulated after Sp1 knockdown in HGC27 and MKN74 cells by Western blotting. These results indicated that Sp1 can significantly regulate the transcription of ITGA1, ITGA2, ITGA5, ITGA6 and ITGA7 by LPPR4.

LPPR4 promotes migration, invasion and adhesion of GC cells by regulating the activity of Sp1

To determine whether LPPR4 could promote migration, invasion of GC cells and adhesion of GC cells to HMrSV5 cells through Sp1, we performed rescue experiments. Sp1 was overexpressed in both HGC27 and MKN74 cells, and overexpression efficiency was detected by Western blotting assays (**Figure 7A**). Transwell migration and matrigel invasion assays showed that Sp1 overexpression enhanced the migration and invasion abilities of GC cells. Sp1 overexpression could restore the migration and invasion ability of HGC27 and MKN74 cells caused by LPPR4 gene knockdown (**Figure 7B, 7C**). In addition, in the case of LPPR4 gene knockdown, overexpression of Sp1 was found to eliminate the reduction of GC cells adhering to HMrSV5 cells (**Figure 7D**, **7E**). These results revealed that knockdown of LPPR4 could suppress migration, invasion and adhesion of GC cells by regulating the expression of Sp1. Taken together, our study demonstrated that LPPR4 could promote peritoneal metastasis via Sp1/integrin α/FAK signaling in GC.

LPPR4 promotes peritoneal metastasis of GC cells in vivo

To investigate whether LPPR4 could promote the peritoneal metastasis of GC cells *in vivo*, a stable LPPR4 knocked-down cell line was established in HGC27 cells. The transfection efficiency of LPPR4 silencing was measured by qRT-PCR and Western blotting (**Figure 8A**, **8B**). HGC27-shNC and HGC27-shLPPR4 cells were injected into the peritoneal cavity of the nude mice to evaluate the effect of LPPR4 on peritoneal implantation *in vivo*. Representative images of GC peritoneal metastasis were selected to present tumor progression in the peritoneum (**Figure 8C**). As shown in **Figure 8D**, HGC27-shLPPR4 cells developed less peritoneal metastatic nodules (2.8±0.4899, N = 5) compared with peritoneal metastatic nodules developed by HGC27-shNC cells (8.6±0.4, N = 5) ($P < 0.001$). Furthermore, the weight of the peritoneal metastatic nodules was significantly heavier for the HGC27-shNC tumors (200.4± 9.182 mg, N = 5) compared with the HGC27-shLPPR4 tumors (59.14±10.94 mg, N = 5) ($P < 0.001$) (**Figure 8E**). Therefore, our findings indicated that LPPR4 fostered peritoneal metastasis of GC cells *in vivo*.

Discussion

Peritoneal dissemination is the most common route of metastasis observed in late-stage GC patients and is considered as the leading cause of death [26]. A distinct feature of peritoneal metastasis in GC is its rapid progression and poor prognosis [27]. Therefore, there is an urgent need to develop novel diagnostic biomarkers and potential treatment targets in GC patients with peritoneal metastases.

In this study, we demonstrated that LPPR4 expression increased in peritoneal metastasis of GC tissues, and predicted a poor clinical outcome in GC patients. In addition, our study provided the first evidence that LPPR4 promoted the migration, invasion and adhesion of GC cells in peritoneal metastasis via Sp1/integrin α/FAK pathway both *in vitro* and *in vivo*. Sp1 was an important determinant of peritoneal metastasis of GC mediated by LPPR4.

Previous studies on LPPR4 focused on the LPPR protein family members. It was revealed that LPPRs could cooperate with each other to form a complex to play an important role in membrane localization and cellular function [28]. However, the functions and mechanisms of LPPRs in tumorigenicity remain unclear. LPPR1 was under-expressed in human adrenal

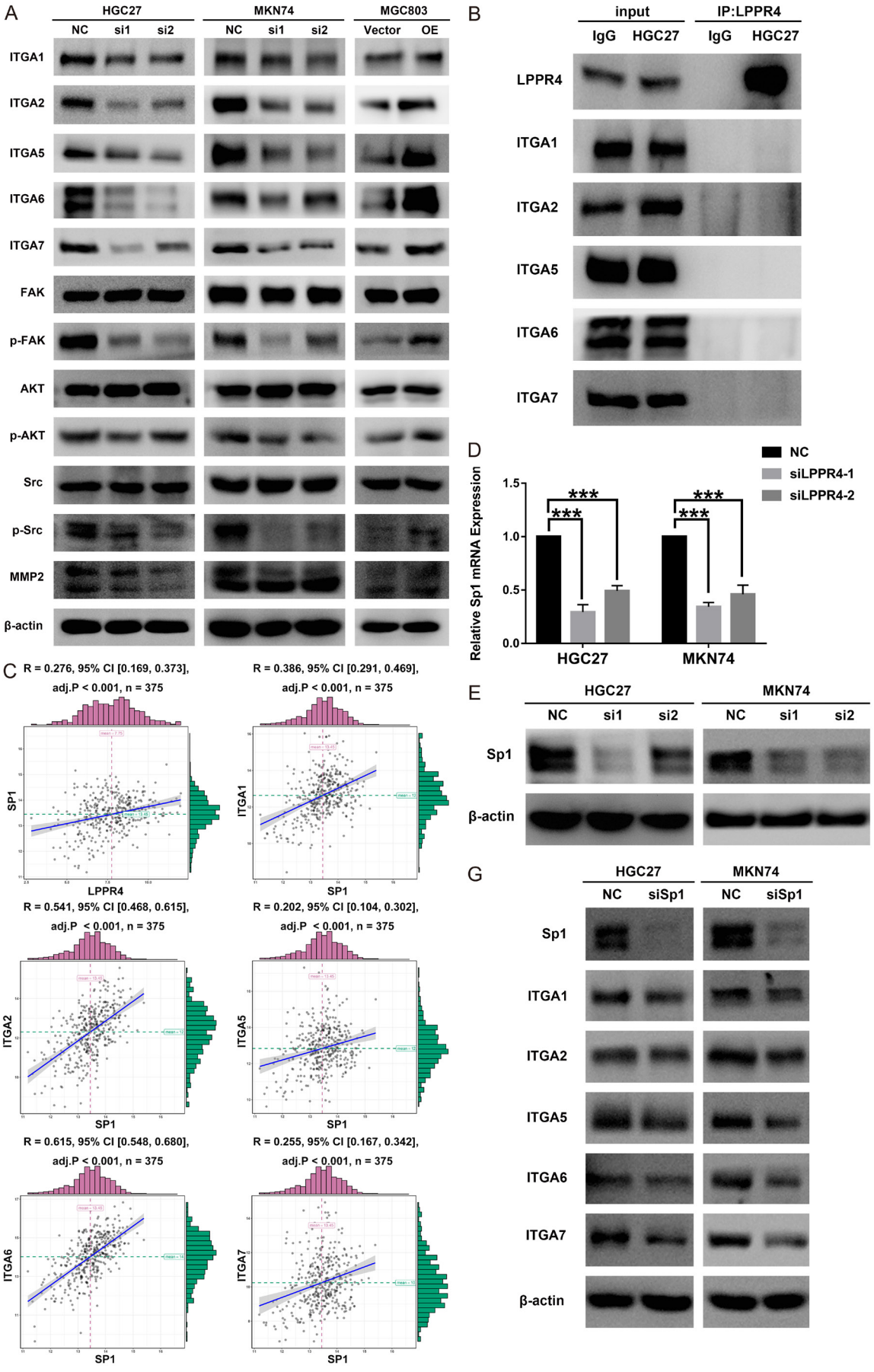
A
HGC27
MKN74
MGC803
NC
si1
si2
Vector
OE
ITGA1
ITGA2
ITGA5
ITGA6
ITGA7
FAK
p-FAK
AKT
p-AKT
Src
p-Src
MMP2
β-actin
B
input
IP:LPPR4
IgG
HGC27
LPPR4
ITGA1
ITGA2
ITGA5
ITGA6
ITGA7
C
R = 0.276, 95% CI [0.169, 0.373], adj.P < 0.001, n = 375
R = 0.386, 95% CI [0.291, 0.469], adj.P < 0.001, n = 375
R = 0.541, 95% CI [0.468, 0.615], adj.P < 0.001, n = 375
R = 0.202, 95% CI [0.104, 0.302], adj.P < 0.001, n = 375
R = 0.615, 95% CI [0.548, 0.680], adj.P < 0.001, n = 375
R = 0.255, 95% CI [0.167, 0.342], adj.P < 0.001, n = 375
SP1
LPPR4
ITGA1
ITGA2
ITGA5
ITGA6
ITGA7
D
NC
siLPPR4-1
siLPPR4-2
Relative Sp1 mRNA Expression
1.5
1.0
0.5
0.0
***
HGC27
MKN74
E
HGC27
MKN74
NC
si1
si2
Sp1
β-actin
G
HGC27
MKN74
NC
siSp1
Sp1
ITGA1
ITGA2
ITGA5
ITGA6
ITGA7
β-actin

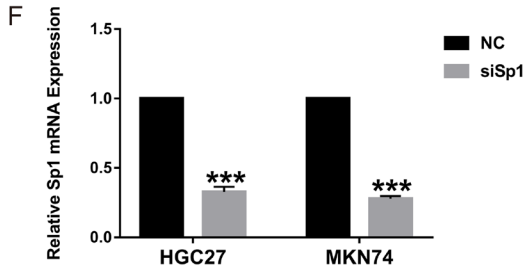

Figure 6. LPPR4 activates transcription of integrin α through Sp1. A. Classical members of integrin family proteins and corresponding downstream genes were assessed by Western blotting in HGC27 and MKN74 cells transfected with siLPPR4 and in MGC803 cells infected with LPPR4 overexpression plasmid. B. Immunoprecipitation using a LPPR4 antibody showed LPPR4 and ITGA1, ITGA2, ITGA5, ITGA6, ITGA7 association. C. Correlation between LPPR4 and Sp1, as well as Sp1 and ITGA1, ITGA2, ITGA5, ITGA6, ITGA7 was performed in human GC tissues based on TCGA-STAD dataset. D. Sp1 mRNA expression levels were tested by qRT-PCR in HGC-27 and MKN74 cells after transfected with siLPPR4. E. Sp1 protein expression levels were detected by Western blotting analysis in HGC27 and MKN74 cells after transfected with siLPPR4. F, G. HGC27 and MKN74 cells were transfected with NC-siRNA and Sp1-siRNA. Sp1 expression levels were detected by qRT-PCR and Western blotting. ITGA1, ITGA2, ITGA5, ITGA6 and ITGA7 protein expression levels were detected by Western blotting analysis in HGC27 and MKN74 cells after transfected with siSp1. β-actin was used as a loading control in Western blotting. Each experiment was repeated at least three times. All the data were expressed as mean ± SD, $***P < 0.001$, based on Student's *t*-test.

cell carcinoma [29]. LPPR4 downregulation has been reported in leukemia [17]. In contrast, up-regulated LPPR2 was associated with drug resistance in human melanoma cell lines [30]. In our study, LPPR4 expression was up-regulated in peritoneal metastasis of GC tissues and elevated LPPR4 expression was correlated with poor prognosis in GC patients.

Most of the previous studies for LPPR4 have reported high levels of expression in neurons, and biological functions in the central nervous system [14, 15]. It was postulated that LPPR4, as a new phospholipid phosphatase, was involved in axonal growth and regenerative sprouting [6]. In addition, LPPR4 regulated spinal density and synaptic plasticity by activating the intracellular protein phosphatase 2A (PP2A)/integrin β1 pathway. Overexpression of LPPR4 promoted the binding of fibronectin (FN) and laminin (LN), and mediated the pathway of CAMs [31]. Consistent with this study, we found that LPPR4 could promote the adhesion of GC cells to HMrSV5 cells *in vitro*. It is well known that the peritoneum mainly consists of a single layer of PMCs. Furthermore, adhesion of cancer cells to PMCs is the crucial step in peritoneal metastasis of GC [32]. Moreover, our results indicated that LPPR4 could promote the migration and invasion of GC cells. Taken together, the results showed that LPPR4 could promote peritoneal metastasis of GC.

Integrins and integrin-related processes have been reported in almost every step of cancer progression, particularly in the metastasis of many cancer types [33]. Integrins play an essential role in modulating cell-extracellular matrix as well as cell-cell interactions in tumor models. Our KEGG and GSEA results indicated that high expression of LPPR4 was correlated with CAMs, focal adhesion and ECM-receptor interaction pathways. Interestingly, we found that the expression of ITGA1, ITGA2, ITGA5, ITGA6 and ITGA7, but not ITGB1, ITGB2, ITGB3, ITGB4 and ITGB5, was significantly decreased by LPPR4 knockdown, indicating that LPPR4 facilitated the activation of integrin α in GC cells. The integrin-correlated adhesion proteins are composed of talin, Src kinase and focal adhesion kinase (FAK). FAK is a non-receptor protein tyrosine kinase which facilitates cancer cell adhesion and metastasis [34]. However, the relationship between LPPR4 and FAK has not previously been elucidated. In our study, LPPR4 gene knockdown was found to down-regulate the expression of p-FAK, p-Src, p-Akt, and the downstream gene MMP2. These results indicated that LPPR4 promoted peritoneal metastasis of GC via the integrin α/FAK pathway.

Another significant finding was that Sp1 acted as a crucial determinant for transcriptional regulation of integrins α by LPPR4. Sp1 is consid-

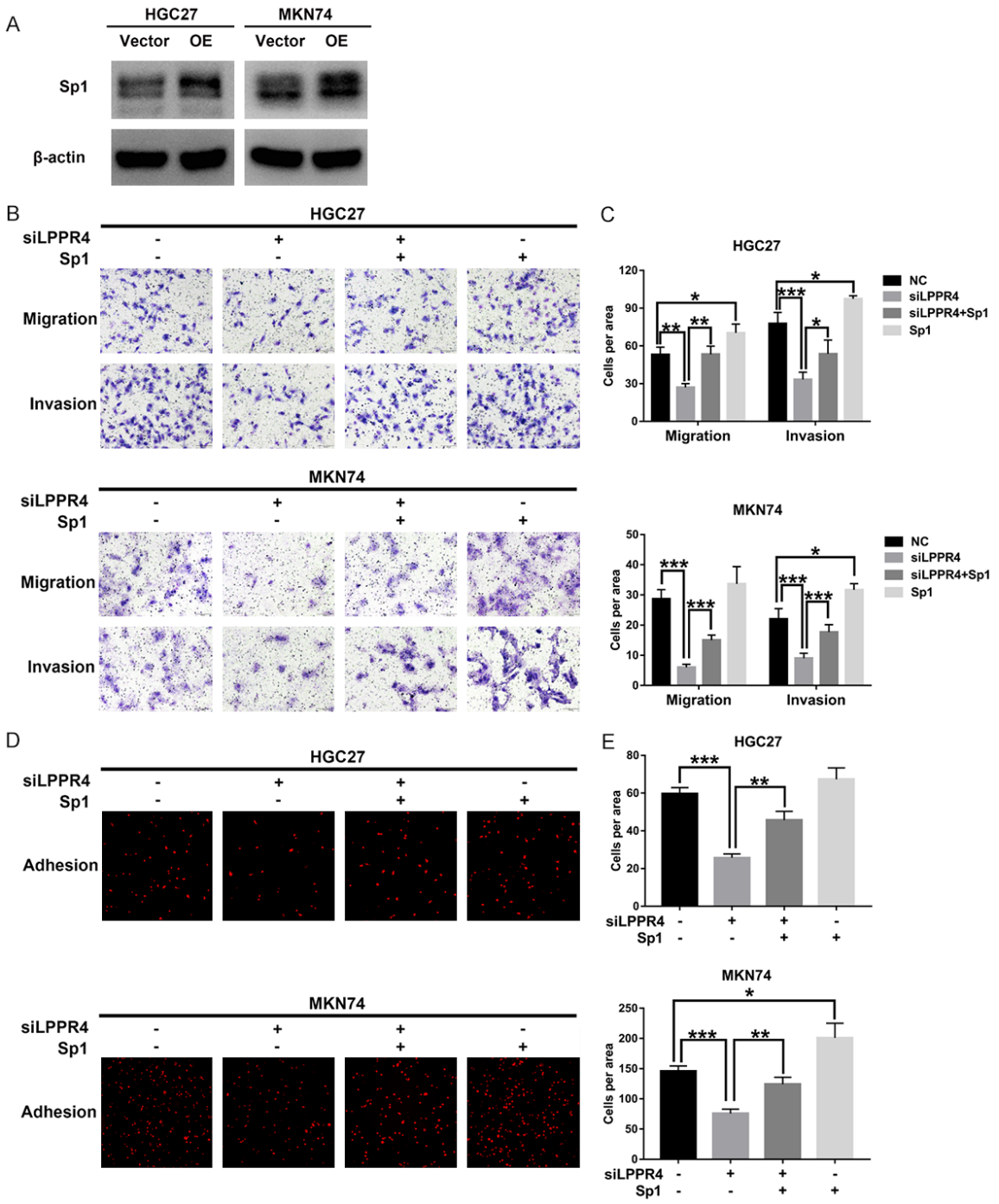

Figure 7. LPPR4 promotes migration, invasion and adhesion of GC cells by regulating the activity of Sp1. A. HGC27 and MKN74 cells were infected with Sp1 overexpression plasmid or the empty vector control. Sp1 expression levels were detected by Western blotting analyses. B, C. Transwell migration and invasion assays of HGC27 and MKN74 cells after treatment with LPPR4 siRNA and/or Sp1 overexpression plasmid. Original magnification, 200×. Scale bar = 100 μm. D, E. Adhesion assays to show HGC27 and MKN74 cells with transient LPPR4 knockdown and/or Sp1 overexpression plasmid adherent to HMrSV5 cells. Original magnification, 100×. Scale bar = 200 μm. β-actin was used as an internal reference for Western blotting. Each experiment was repeated at least three times. All the data were expressed as mean ± SD, $*P < 0.05$, $**P < 0.01$, $***P < 0.001$, based on Student's *t*-test.

ered as a classical transcription factor and plays an important role in metabolism, cell growth regulation, cell death, and cancer progression [35]. Overexpressed Sp1 is involved in

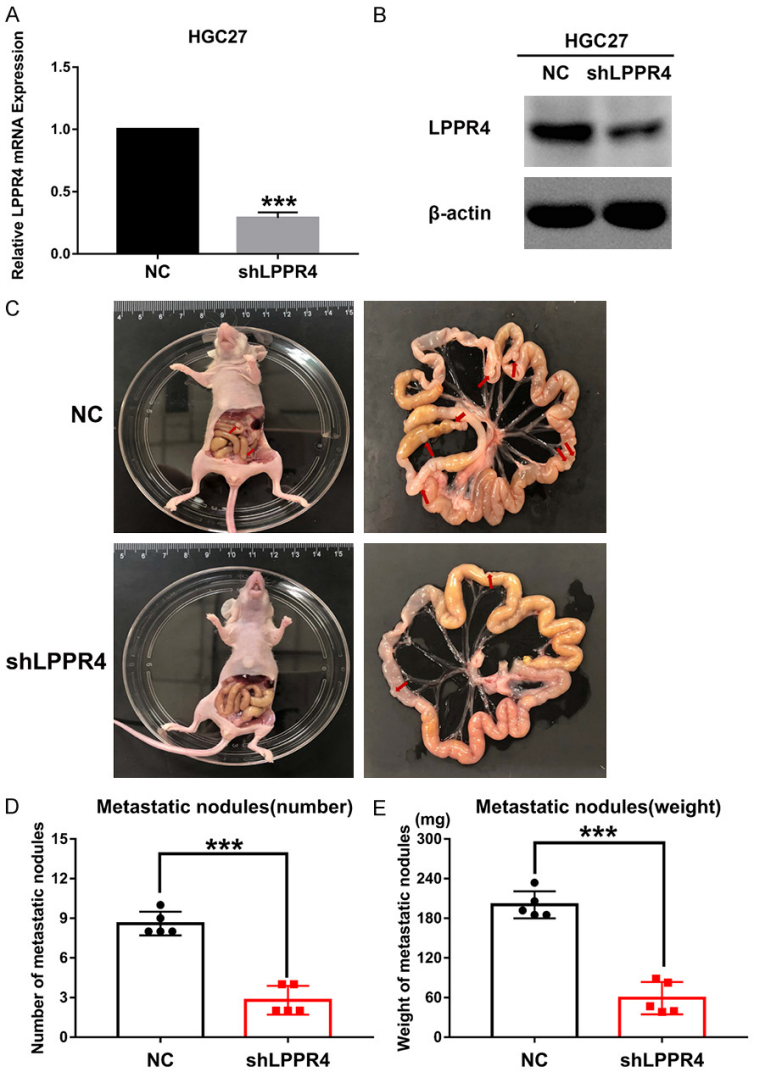

Figure 8. LPPR4 promotes peritoneal metastasis of GC cells *in vivo*. A, B. HGC27 cells were infected with NC or LPPR4-shRNA lentiviral particles. LPPR4 expression levels were detected by qRT-PCR and Western blotting analyses. C. Representative images of the macroscopic appearance of peritoneal metastatic nodules (red arrows) in nude mice treated with intraperitoneal injection of HGC27 cells stably infected with NC or LPPR4-shRNA lentiviral particles (N = 5 per group). D. The total number of peritoneal metastatic nodules in respective group. E. The total weight of peritoneal metastatic nodules in respective group. Each experiment was repeated at least three times. All the data were presented as mean ± SD, ***$P < 0.001$, based on Student's *t*-test.

many cancers including breast, gastric, liver, thyroid and pancreatic cancers [36-40]. Several previous studies have demonstrated the importance of Sp1 in the regulation of integrins [24, 25, 36]. Our results showed that Sp1 acted as an important transcription factor for the expression of integrin α by LPPR4. LPPR4 promoted GC cell migration, invasion and adhesion to HMrSV5 cells through Sp1. Overall, our data revealed that LPPR4 promoted GC peritoneal metastasis via the Sp1/integrin α/FAK pathway.

Our present study has several limitations in explaining the molecular mechanisms of LPPR4. The bioinformatics functional analysis of LPPR4 could not comprehensively reveal the biological function of LPPR4. It would be worthwhile to use LPPR4 overexpression or knockout microarrays in GC cells. Additionally, a further study of the mechanisms by which LPPR4 regulates Sp1 is needed.

In summary, the present study suggests, for the first time, that the expression of LPPR4 is significantly overexpressed in peritoneal metastasis of GC. The increased expression of LPPR4 correlates with shorter overall survival in GC patients. Moreover, LPPR4 promotes migration, invasion and adhesion of GC cells through the Sp1/integrin α/FAK signaling pathway. LPPR4 may serve as a potential biomarker for the diagnosis and prediction of prognosis of GC peritoneal metastasis. Targeting LPPR4 may be a promising strategy for the treatment of peritoneal metastasis of GC patients.

Acknowledgements

This work was supported by National Science and Technology Major Project of the Ministry of Science and Technology of China (No. 2017ZX09304025); National Natural Science Foundation of China (NO. 81972331, NO. 81972751, NO. 81572374); The Key Research and Development Program of Liaoning Province (2018225060); Science and Technology Plan Project of Shenyang city (1900940); Science and Technology Plan Project of Liaoning Province (NO. 2013225585); The National Key

Research and Development Program of China (NO. 2017YFC1308900).

Disclosure of conflict of interest

None.

Address correspondence to: Xiujuan Qu and Yunpeng Liu, Department of Medical Oncology, The First Hospital of China Medical University, Shenyang, China; Key Laboratory of Anticancer Drugs and Biotherapy of Liaoning Province, The First Hospital of China Medical University, Shenyang, China; Liaoning Province Clinical Research Center for Cancer, The First Hospital of China Medical University, Shenyang, China; Key Laboratory of Precision Diagnosis and Treatment of Gastrointestinal Tumors, Ministry of Education, The First Hospital of China Medical University, Shenyang, China. Tel: +86-24-83282312; Fax: +86-24-83282312; E-mail: xiujuanqu@yahoo.com (XJQ); ypliu@cmu.edu.cn (YPL)

References

[1] Siegel RL, Miller KD and Jemal A. Cancer statistics, 2018. CA Cancer J Clin 2018; 68: 7-30.

[2] Ajani JA, D'Amico TA, Almhanna K, Bentrem DJ, Chao J, Das P, Denlinger CS, Fanta P, Farjah F, Fuchs CS, Gerdes H, Gibson M, Glasgow RE, Hayman JA, Hochwald S, Hofstetter WL, Ilson DH, Jaroszewski D, Johung KL, Keswani RN, Kleinberg LR, Korn WM, Leong S, Linn C, Lockhart AC, Ly QP, Mulcahy MF, Orringer MB, Perry KA, Poultsides GA, Scott WJ, Strong VE, Washington MK, Weksler B, Willett CG, Wright CD, Zelman D, McMillian N and Sundar H. Gastric cancer, version 3.2016, NCCN clinical practice guidelines in oncology. J Natl Compr Canc Netw 2016; 14: 1286-1312.

[3] McLean MH and El-Omar EM. Genetics of gastric cancer. Nat Rev Gastroenterol Hepatol 2014; 11: 664-674.

[4] Wang FH, Shen L, Li J, Zhou ZW, Liang H, Zhang XT, Tang L, Xin Y, Jin J, Zhang YJ, Yuan XL, Liu TS, Li GX, Wu Q, Xu HM, Ji JF, Li YF, Wang X, Yu S, Liu H, Guan WL and Xu RH. The Chinese Society of Clinical Oncology (CSCO): clinical guidelines for the diagnosis and treatment of gastric cancer. Cancer Commun (Lond) 2019; 39: 10.

[5] Rau B, Brandl A, Thuss-Patience P, Bergner F, Raue W, Arnold A, Horst D, Pratschke J and Biebl M. The efficacy of treatment options for patients with gastric cancer and peritoneal metastasis. Gastric Cancer 2019; 22: 1226-1237.

[6] Brauer AU, Savaskan NE, Kuhn H, Prehn S, Ninnemann O and Nitsch R. A new phospholipid phosphatase, PRG-1, is involved in axon growth and regenerative sprouting. Nat Neurosci 2003; 6: 572-578.

[7] Broggini T, Nitsch R and Savaskan NE. Plasticity-related gene 5 (PRG5) induces filopodia and neurite growth and impedes lysophosphatidic acid- and nogo-A-mediated axonal retraction. Mol Biol Cell 2010; 21: 521-537.

[8] Savaskan NE, Brauer AU and Nitsch R. Molecular cloning and expression regulation of PRG-3, a new member of the plasticity-related gene family. Eur J Neurosci 2004; 19: 212-220.

[9] Sciorra VA and Morris AJ. Roles for lipid phosphate phosphatases in regulation of cellular signaling. Biochim Biophys Acta 2002; 1582: 45-51.

[10] Brindley DN. Lipid phosphate phosphatases and related proteins: signaling functions in development, cell division, and cancer. J Cell Biochem 2004; 92: 900-912.

[11] Xu Y, Gaudette DC, Boynton JD, Frankel A, Fang XJ, Sharma A, Hurteau J, Casey G, Goodbody A, Mellors A, Holub BJ and Mills GB. Characterization of an ovarian cancer activating factor in ascites from ovarian cancer patients. Clin Cancer Res 1995; 1: 1223-1232.

[12] Xiao YJ, Schwartz B, Washington M, Kennedy A, Webster K, Belinson J and Xu Y. Electrospray ionization mass spectrometry analysis of lysophospholipids in human ascitic fluids: comparison of the lysophospholipid contents in malignant vs nonmalignant ascitic fluids. Anal Biochem 2001; 290: 302-313.

[13] Hong G, Baudhuin LM and Xu Y. Sphingosine-1-phosphate modulates growth and adhesion of ovarian cancer cells. FEBS Lett 1999; 460: 513-518.

[14] Trimbuch T, Beed P, Vogt J, Schuchmann S, Maier N, Kintscher M, Breustedt J, Schuelke M, Streu N, Kieselmann O, Brunk I, Laube G, Strauss U, Battefeld A, Wende H, Birchmeier C, Wiese S, Sendtner M, Kawabe H, Kishimoto-Suga M, Brose N, Baumgart J, Geist B, Aoki J, Savaskan NE, Brauer AU, Chun J, Ninnemann O, Schmitz D and Nitsch R. Synaptic PRG-1 modulates excitatory transmission via lipid phosphate-mediated signaling. Cell 2009; 138: 1222-1235.

[15] Tokumitsu H, Hatano N, Tsuchiya M, Yurimoto S, Fujimoto T, Ohara N, Kobayashi R and Sakagami H. Identification and characterization of PRG-1 as a neuronal calmodulin-binding protein. Biochem J 2010; 431: 81-91.

[16] Gaaya A, Poirier O, Mougenot N, Hery T, Atassi F, Marchand A, Saulnier-Blache JS, Amour J, Vogt J, Lompre AM, Soubrier F and Nadaud S. Plasticity-related gene-1 inhibits lysophosphatidic acid-induced vascular smooth muscle cell migration and proliferation and prevents neointima formation. Am J Physiol Cell Physiol 2012; 303: C1104-1114.

[17] Klener P, Szynal M, Cleuter Y, Merimi M, Duvillier H, Lallemand F, Bagnis C, Griebel P, Sotiriou C, Burny A, Martiat P and Van den Broeke A. Insights into gene expression changes impacting B-cell transformation: cross-species micro-

array analysis of bovine leukemia virus tax-responsive genes in ovine B cells. J Virol 2006; 80: 1922-1938.
[18] Rougier JP, Moullier P, Piedagnel R and Ronco PM. Hyperosmolality suppresses but TGF beta 1 increases MMP9 in human peritoneal mesothelial cells. Kidney Int 1997; 51: 337-347.
[19] Deng G, Qu J, Zhang Y, Che X, Cheng Y, Fan Y, Zhang S, Na D, Liu Y and Qu X. Gastric cancer-derived exosomes promote peritoneal metastasis by destroying the mesothelial barrier. FEBS Lett 2017; 591: 2167-2179.
[20] Zhang L, Li Z, He W, Xu L, Wang J, Shi J and Sheng M. Effects of astragaloside IV against the TGF-beta1-induced epithelial-to-mesenchymal transition in peritoneal mesothelial cells by promoting Smad 7 expression. Cell Physiol Biochem 2015; 37: 43-54.
[21] Li Q, Li B, Li Q, Wei S, He Z, Huang X, Wang L, Xia Y, Xu Z, Li Z, Wang W, Yang L, Zhang D and Xu Z. Exosomal miR-21-5p derived from gastric cancer promotes peritoneal metastasis via mesothelial-to-mesenchymal transition. Cell Death Dis 2018; 9: 854.
[22] Hamidi H and Ivaska J. Every step of the way: integrins in cancer progression and metastasis. Nat Rev Cancer 2018; 18: 533-548.
[23] Mathelier A, Fornes O, Arenillas DJ, Chen CY, Denay G, Lee J, Shi W, Shyr C, Tan G, Worsley-Hunt R, Zhang AW, Parcy F, Lenhard B, Sandelin A and Wasserman WW. JASPAR 2016: a major expansion and update of the open-access database of transcription factor binding profiles. Nucleic Acids Res 2016; 44: D110-115.
[24] Kim ES, Kim SY, Koh M, Lee HM, Kim K, Jung J, Kim HS, Moon WK, Hwang S and Moon A. C-reactive protein binds to integrin alpha2 and Fcgamma receptor I, leading to breast cell adhesion and breast cancer progression. Oncogene 2018; 37: 28-38.
[25] Nam EH, Lee Y, Park YK, Lee JW and Kim S. ZEB2 upregulates integrin alpha5 expression through cooperation with Sp1 to induce invasion during epithelial-mesenchymal transition of human cancer cells. Carcinogenesis 2012; 33: 563-571.
[26] Dahdaleh FS and Turaga KK. Evolving treatment strategies and outcomes in advanced gastric cancer with peritoneal metastasis. Surg Oncol Clin N Am 2018; 27: 519-537.
[27] Mikula-Pietrasik J, Uruski P, Tykarski A and Ksiazek K. The peritoneal "soil" for a cancerous "seed": a comprehensive review of the pathogenesis of intraperitoneal cancer metastases. Cell Mol Life Sci 2018; 75: 509-525.
[28] Yu P, Agbaegbu C, Malide DA, Wu X, Katagiri Y, Hammer JA and Geller HM. Cooperative interactions of LPPR family members in membrane localization and alteration of cellular morphology. J Cell Sci 2015; 128: 3210-3222.
[29] Barzon L, Masi G, Fincati K, Pacenti M, Pezzi V, Altavilla G, Fallo F and Palu G. Shift from Conn's syndrome to Cushing's syndrome in a recurrent adrenocortical carcinoma. Eur J Endocrinol 2005; 153: 629-636.
[30] Tanic N, Brkic G, Dimitrijevic B, Dedovic-Tanic N, Gefen N, Benharroch D and Gopas J. Identification of differentially expressed mRNA transcripts in drug-resistant versus parental human melanoma cell lines. Anticancer Res 2006; 26: 2137-2142.
[31] Liu X, Huai J, Endle H, Schluter L, Fan W, Li Y, Richers S, Yurugi H, Rajalingam K, Ji H, Cheng H, Rister B, Horta G, Baumgart J, Berger H, Laube G, Schmitt U, Schmeisser MJ, Boeckers TM, Tenzer S, Vlachos A, Deller T, Nitsch R and Vogt J. PRG-1 regulates synaptic plasticity via Intracellular PP2A/beta1-integrin signaling. Dev Cell 2016; 38: 275-290.
[32] Rynne-Vidal A, Jimenez-Heffernan JA, Fernandez-Chacon C, Lopez-Cabrera M and Sandoval P. The mesothelial origin of carcinoma associated-fibroblasts in peritoneal metastasis. Cancers (Basel) 2015; 7: 1994-2011.
[33] Raab-Westphal S, Marshall JF and Goodman SL. Integrins as therapeutic targets: successes and cancers. Cancers (Basel) 2017; 9.
[34] Kleinschmidt EG and Schlaepfer DD. Focal adhesion kinase signaling in unexpected places. Curr Opin Cell Biol 2017; 45: 24-30.
[35] Black AR, Black JD and Azizkhan-Clifford J. Sp1 and kruppel-like factor family of transcription factors in cell growth regulation and cancer. J Cell Physiol 2001; 188: 143-160.
[36] Hedrick E, Li X and Safe S. Penfluridol represses integrin expression in breast cancer through induction of reactive oxygen species and downregulation of Sp transcription factors. Mol Cancer Ther 2017; 16: 205-216.
[37] Gong L, Wen T, Li Z, Wang Y, Wang J, Che X, Liu Y and Qu X. TNPO2 operates downstream of DYNC1I1 and promotes gastric cancer cell proliferation and inhibits apoptosis. Cancer Med 2019; 8: 7299-7312.
[38] Wu W, Dong YW, Shi PC, Yu M, Fu D, Zhang CY, Cai QQ, Zhao QL, Peng M, Wu LH and Wu XZ. Regulation of integrin alphaV subunit expression by sulfatide in hepatocellular carcinoma cells. J Lipid Res 2013; 54: 936-952.
[39] Chiefari E, Brunetti A, Arturi F, Bidart JM, Russo D, Schlumberger M and Filetti S. Increased expression of AP2 and Sp1 transcription factors in human thyroid tumors: a role in NIS expression regulation? BMC Cancer 2002; 2: 35.
[40] Jiang NY, Woda BA, Banner BF, Whalen GF, Dresser KA and Lu D. Sp1, a new biomarker that identifies a subset of aggressive pancreatic ductal adenocarcinoma. Cancer Epidemiol Biomarkers Prev 2008; 17: 1648-1652.

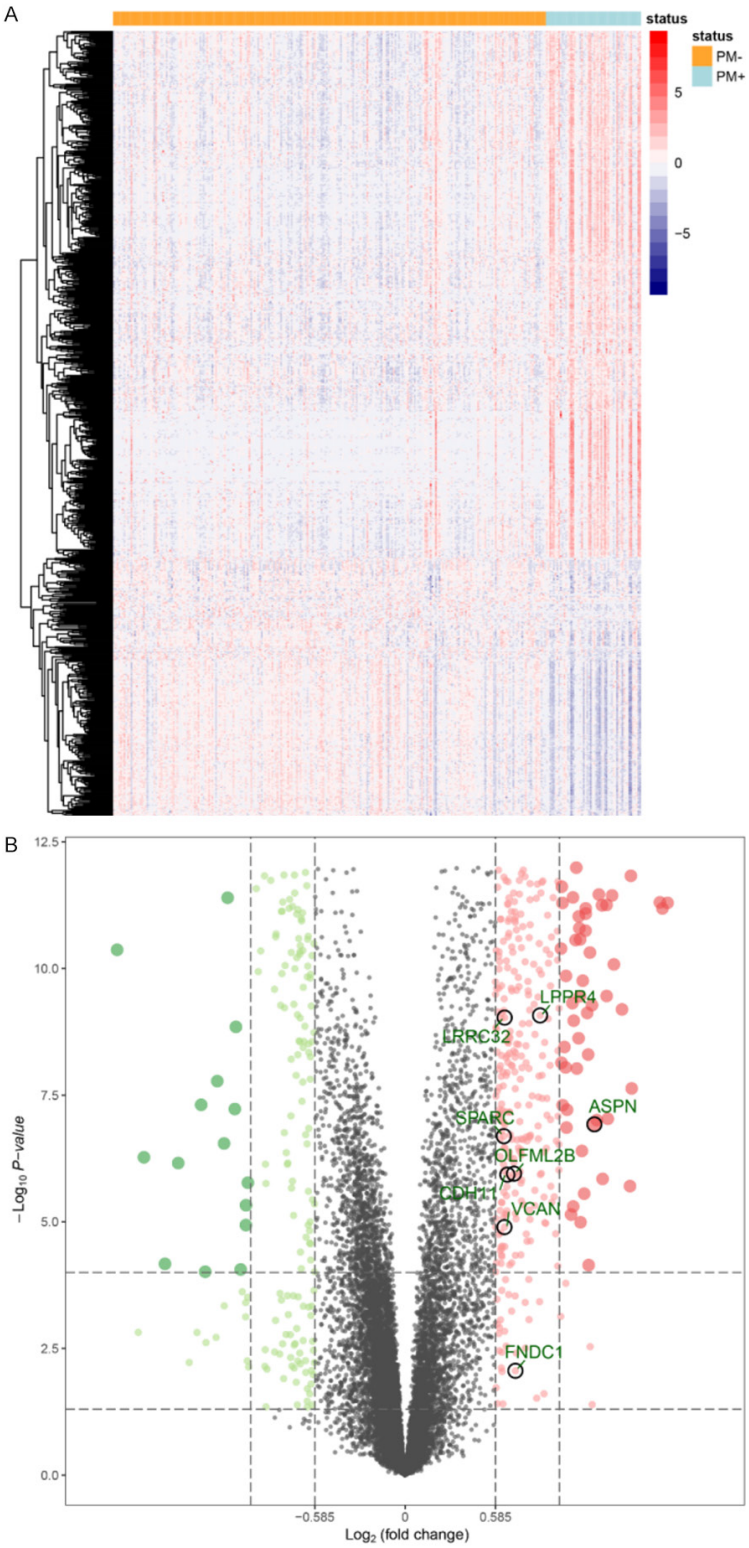

Figure S1. A, B. The heatmap and volcano map of the DEGs between peritoneal relapse tissues and non-peritoneal relapse tissues of GSE62254 cohort respectively.

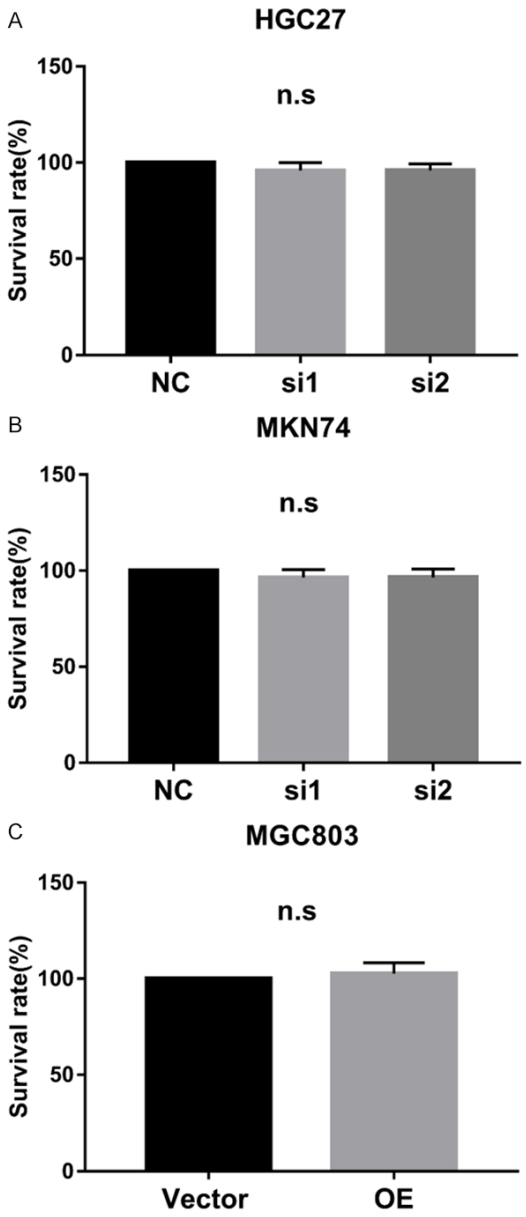

Figure S2. A-C. The cell viability of GC cell lines during migration and invasion was carried out by MTT assays. Each experiment was repeated at least three times. All the data were presented as mean ± SD, n.s, no significance.

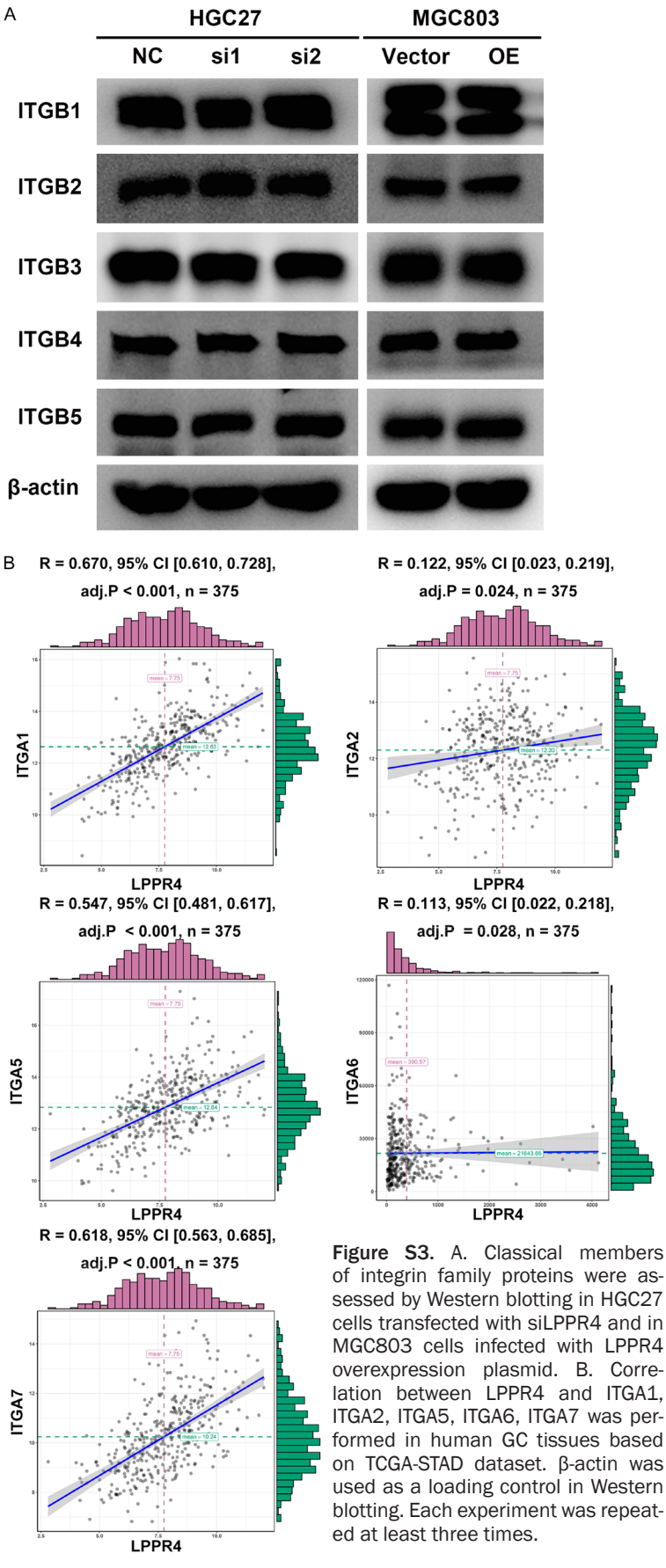

Figure S3. A. Classical members of integrin family proteins were assessed by Western blotting in HGC27 cells transfected with siLPPR4 and in MGC803 cells infected with LPPR4 overexpression plasmid. B. Correlation between LPPR4 and ITGA1, ITGA2, ITGA5, ITGA6, ITGA7 was performed in human GC tissues based on TCGA-STAD dataset. β-actin was used as a loading control in Western blotting. Each experiment was repeated at least three times.